

Supporting Information

Facet dependent pairwise addition of hydrogen over Pd nanocrystal catalysts revealed by NMR using para-hydrogen-induced polarization

Weiyu Wang^a, Jun Xu^{a,}, Yanxi Zhao^b, Guodong Qi^a, Qiang Wang^a, Chao Wang^a, Jinlin Li^b, Feng Deng^{a,*}*

^a National Center for Magnetic Resonance in Wuhan, State Key Laboratory of Magnetic Resonance and Atomic and Molecular Physics, Wuhan Institute of Physics and Mathematics, Chinese Academy of Sciences, Wuhan 430071, China.

^bKey Laboratory of Catalysis and Materials Science of the State Ethnic Affairs Commission & Ministry of Education, South-Central University for Nationalities, Wuhan 430074, China.

Materials and Sample Preparation

The Na_2PdCl_4 (99.99%), Poly (vinyl pyrrolidone) (PVP, $M_w \approx 55\ 000$), $\text{FeO}(\text{OH})$ (catalog number 371254, 30-50 mesh), d-DMSO (99.9 atom % D) were purchased from Sigma-Aldrich. L-ascorbic acid (AA), KCl, KBr, formaldehyde were purchased from Sinopharm Chemical Reagent Co. Ltd. All the reagents were used directly.

On the basis of the previous reports¹, Pd nanocubes and octahedrons were synthesized by a solution-phase method with PVP as stabilizer. Briefly, the Pd nanocubes were synthesized as follows: a 25 ml flask was filled with an 8.0 mL aqueous solution containing 105 mg PVP, 60 mg AA, and different amount of KBr and KCl, then it was heated at 353 K for 10 min under magnetic stirring in air. After heating, a 3 mL aqueous solution containing 57 mg Na_2PdCl_4 was added into the flask, and then the flask was capped and allowed to react for 3 h. The size of the synthesized nanocubes was controlled by adding different amount of KBr and KCl. In our experiments, 75 mg KBr and 141 mg KCl produced nanocubes with an average diameter of 8.7 nm (CUB-8); 300 mg KBr produced nanocubes with an average diameter of 11.1 nm (CUB-11), and 400 mg KBr produced nanocubes with an average diameter of 14.4 nm (CUB-14).

Pd nanocrystals with different shapes were prepared by using Pd nanocubes as seeds. Briefly, 8.0 mL aqueous solution containing 105 mg PVP, 100 μL HCHO, and 0.3 mL of an aqueous suspension ($1.8\ \text{mg mL}^{-1}$ in concentration) of cubic seeds that were synthesized above were filled into a 25 ml flask, then it was capped and heated at 333K with magnetic stirring for 5 min. Then, 3 mL of an aqueous solution containing

2.9 mg Na_2PdCl_4 was added quickly. After capped, the whole solution was allowed to react for 3 h. Different amount of Na_2PdCl_4 will lead to different shapes of the synthesized nanocrystals. Using CUB-11 nanocubes as seeds, 2.9 mg Na_2PdCl_4 produced cuboctahedrons with an average diameter of 19.4 nm (COT-19), 5.8 mg Na_2PdCl_4 produced truncated octahedrons with an average diameter of 23.6 nm (TOT-23) and 11.6 mg Na_2PdCl_4 produced octahedrons with an average diameter of 27.9 nm (OCT-27). We also synthesized two series of octahedrons (OCT) with different sizes by using Pd nanocubes (CUB) seeds with different sizes: OCT-17 with an average diameter of 17.9 nm was synthesized with CUB-8 and OCT-34 with an average diameter of 34.3 nm was synthesized with CUB-14. To remove the excess PVP stabilizer, all the synthesized products were washed and collected by centrifugation with acetone (1/3 v/v solution/acetone) three times, then the final products were re-dispersed in water before used for the reactions.

Hydrogenation experiments

A continuous stream of H_2 gas containing approximately 50% parahydrogen (p- H_2) spin isomer is produced by passing normal hydrogen in a 1:3 mixture of para- H_2 and ortho- H_2 (n- H_2) through a copper coil filled with $\text{FeO}(\text{OH})$ (Sigma-Aldrich, 30-50 mesh) and immersed in liquid N_2 (77 K).²

MBY hydrogenation reactions were carried out in a 10 mm glass NMR tube, which was loaded with 1.5 mL d-DMSO, 0.5 mL MBY (98%) and 0.1 mL Pd nanocrystals aqueous solution (0.2 mg). The PHIP experiments were performed with PASADENA approach³. Before the PASADENA experiments, the NMR tube containing catalysts

and MBY mixture was first charged with p-H₂ to 2-4 bar, and then transferred into the NMR spectrometer. The p-H₂ with a flow rate of 70 mL/min was bubbled through the mixture via a Teflon capillary extended to the bottom of the NMR tube. The reactions were carried out at temperature of 343-373 K. All the ¹H NMR spectra were recorded by on a Bruker Avance III 600 NMR spectrometer with a ¹H resonance frequency of 599.94 MHz. A $\pi/4$ rf pulse was used to maximize the PASADENA NMR signals.⁴ The ¹H PHIP NMR spectra were acquired after the stop of p-H₂ flow to avoid magnetic field inhomogeneities induced by bubbles in the reaction mixture.

SEM and TEM measurements

For SEM and TEM characterizations, samples were prepared by dropping a suspension of the nanocrystals in water on silicon substrates and carbon-coated copper grids, respectively, followed by drying under ambient conditions. SEM images were obtained using a HITACHI SU8010 field-emission scanning electron microscope operated at an accelerating voltage of 15 kV. TEM images were obtained on a FEI Tecnai G² 20 S-Twin instrument at an accelerating voltage of 200 kV.

Calculations of enhancement factor and pairwise selectivity

All polarization values obtained via hydrogenation reactions were calculated with the assumption that MBE is the only product for MBY conversion. The signal enhancement factors were calculated by comparing the polarized spectra and thermally polarized NMR spectra after the complete relaxation of hyperpolarization. The calculation followed the reported method⁵. The experimental signal enhancement factor was evaluated by comparing the CH multiplets in the NMR spectra of MBE

(signal H_e in Figure 1) produced with the use of $n-H_2$ and $p-H_2$. The integral of the entire CH multiplets in the case of $n-H_2$ was considered, while the positive half of the antiphase multiplets was integrated in the case of $p-H_2$. Accordingly, the ratio of the corresponding integrals ($p-H_2/n-H_2$) as the signal enhancement factor can be determined. Pairwise selectivity of $p-H_2$ addition describes the fraction of protons from the same hydrogen molecule with respect to the total added protons in the hydrogenated substrate. It can be calculated by the ratio of the experimental and theoretical enhancement factors. The theoretical enhancement factor is calculated according to the report of Koptug⁶ and Bowers⁷. In our experiments, the pairwise selectivity was calculated based on the CH multiplets and the pattern of the multiplets that was taken into account. The theoretical pattern of line intensities for the CH group coupled to two methene protons in MBE is (1, 1, 1, 1) for the thermally polarized NMR spectrum and (1, -1, 1, -1) for the PASADENA NMR spectrum.

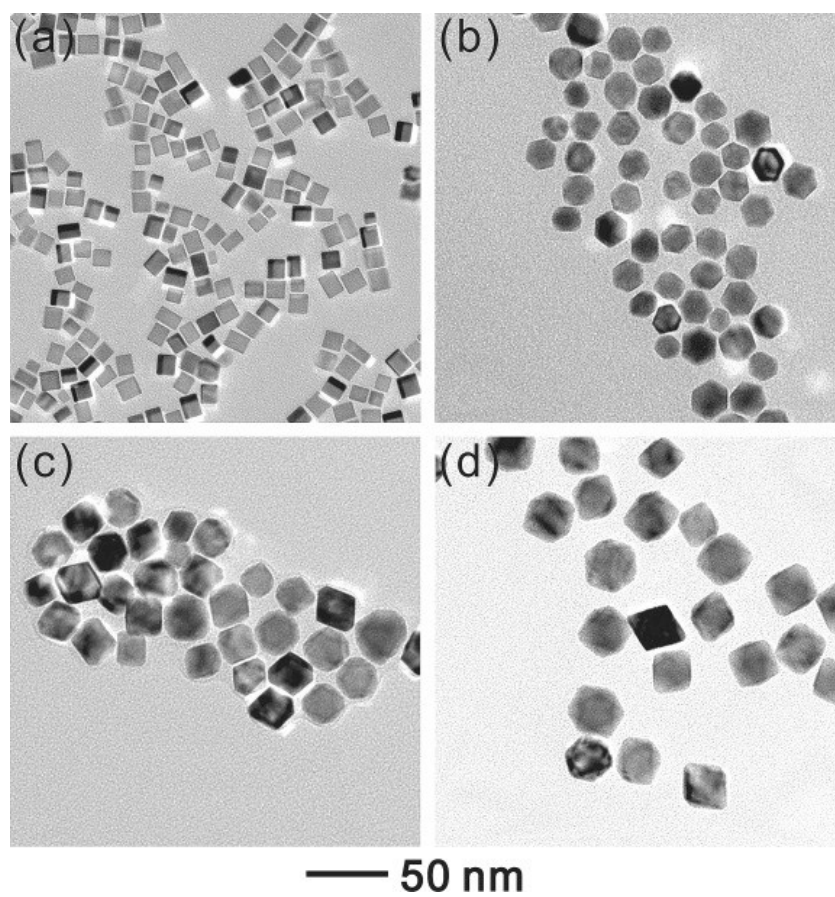


Figure S1. TEM images of Pd nanocrystals: (a) 11.1 nm cubes, (b) 19.4 nm cuboctahedrons, (c) 23.6 nm truncated octahedrons, and (d) 27.9 nm octahedrons.

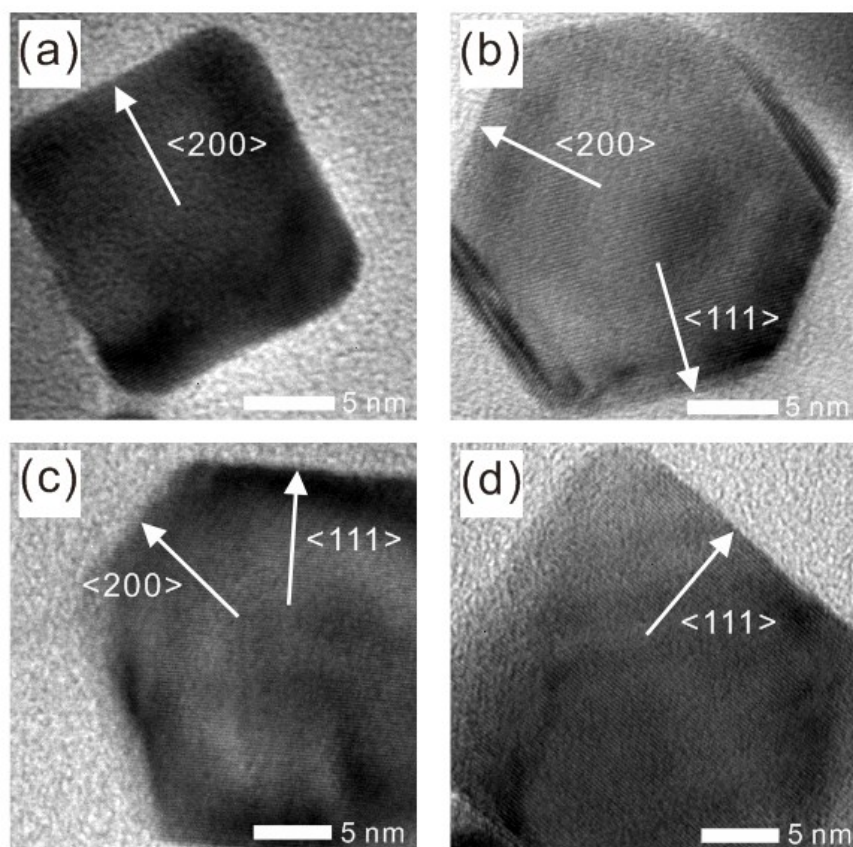


Figure S2. HRTEM images of the Pd nanocrystals: (a) 11.1 nm cubes, (b) 19.4 nm cuboctahedrons, (c) 23.6 nm truncated octahedrons, and (d) 27.9 nm octahedrons.

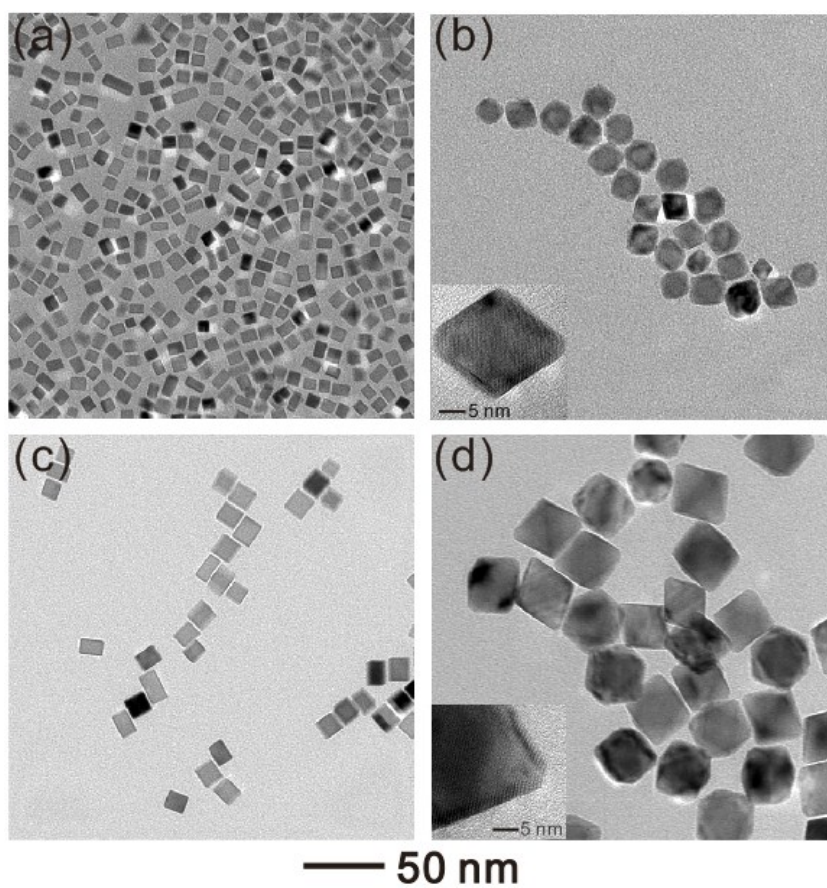


Figure S3. TEM images of Pd nanocrystals: (a) 8.7 nm cubes, (b) 17.9 nm octahedrons, (c) 14.4 nm cubes, and (d) 34.3 nm octahedrons. The insert shows the high resolution images.

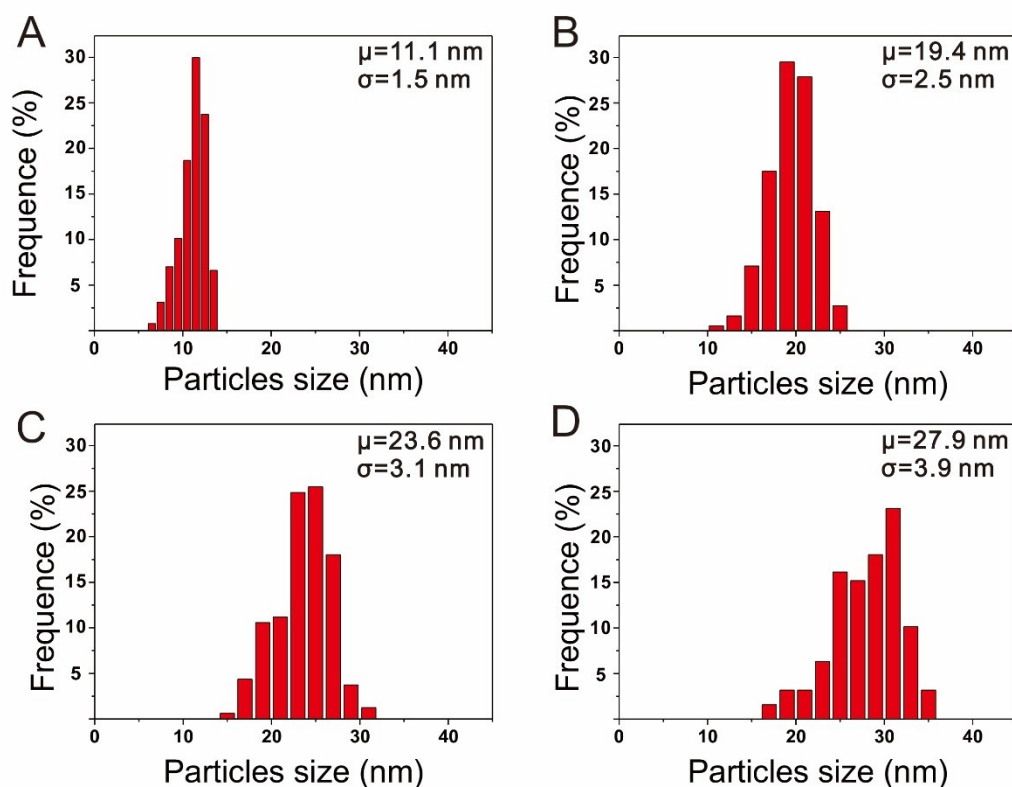


Figure S4. Particle size distributions of Pd nanocrystals: (a) CUB-11, (b) COT-19, (c) TOT-23 and (d) OCT-27. More than 95% of the nanocrystals exhibit the predominant shape. μ represents the average particle size and σ represents the standard deviation of the particles.

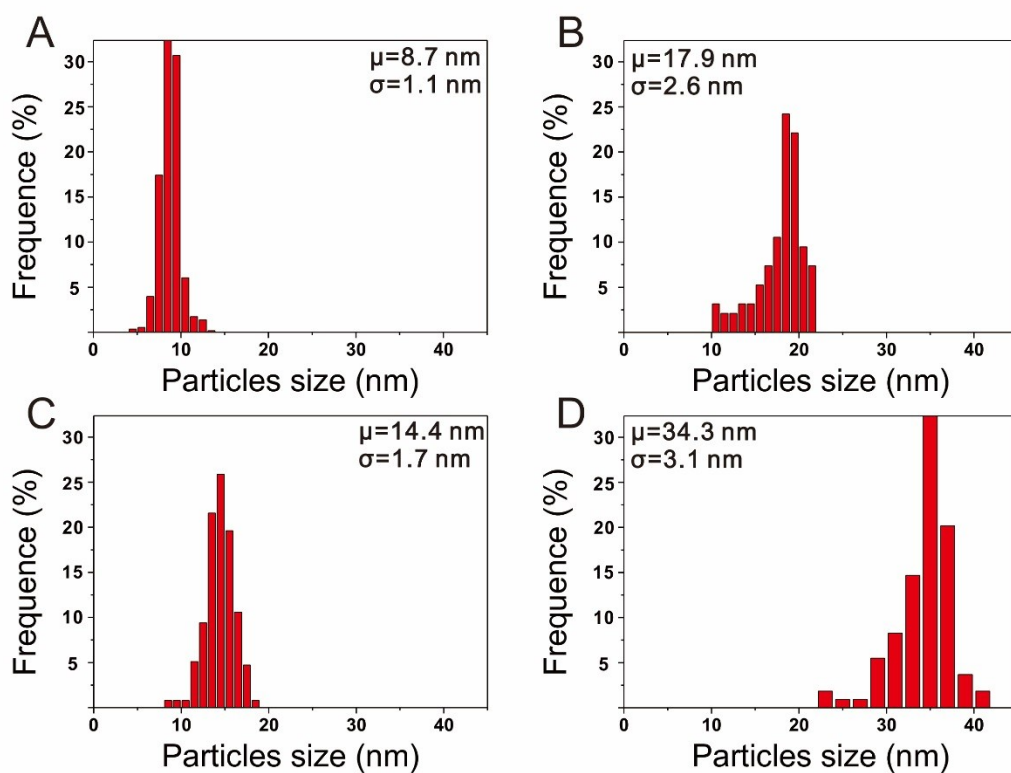


Figure S5. Particle size distributions of Pd nanocrystals: (a) CUB-8, (b) OCT-17, (c) CUB-14 and (d) OCT-34. More than 95% of the nanocrystals exhibit the predominant shape. μ represents the average particle size and σ represents the standard deviation of the particles.

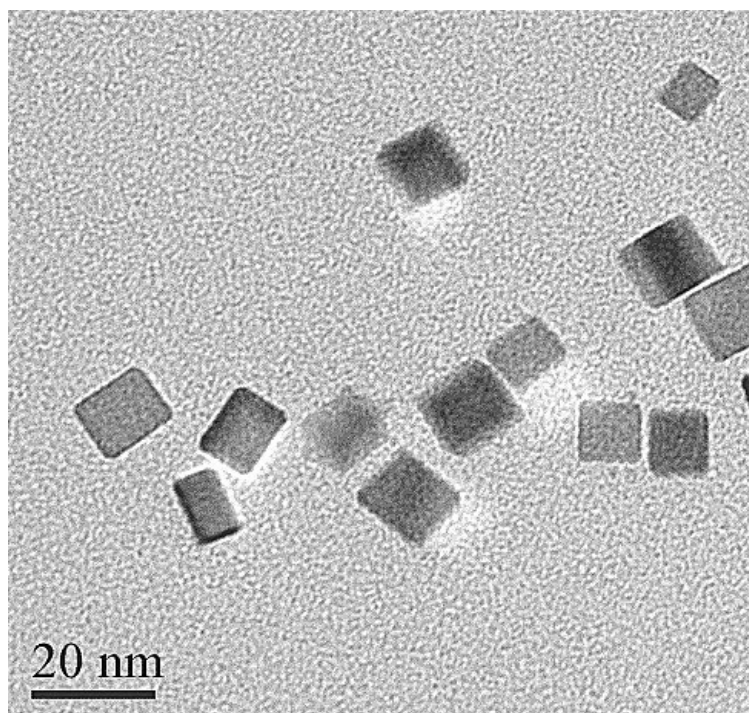


Figure S6. TEM image of cubic nanocrystals collected after the hydrogenation reaction at 353.2 K and 4 bar. The Pd morphology was well maintained.

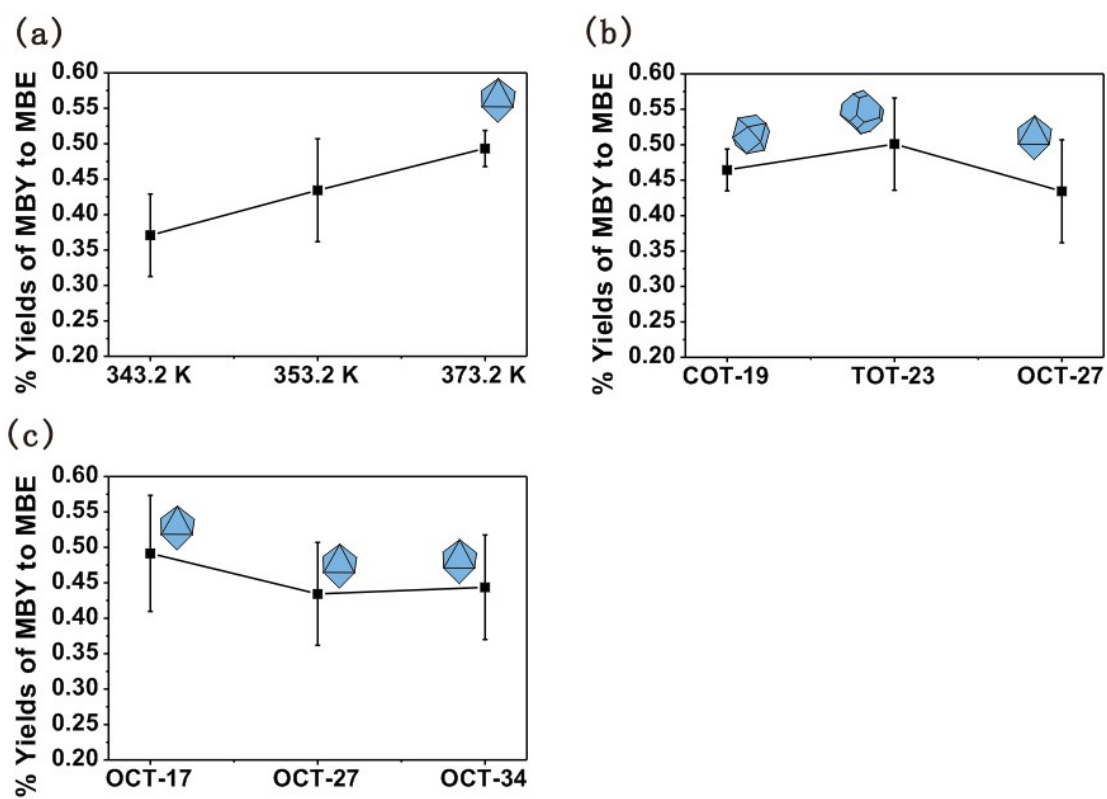


Figure S7. The yields of MBY to MBE on (a) Pd OCT-27 catalyst at different reaction temperatures, (b) Pd nanocrystals in different shapes (COT-19, TOT-23 and OCT-27) at 353 K and (c) Pd octahedrons in different sizes (OCT-17, OCT-27 and OCT-34) at 353 K.

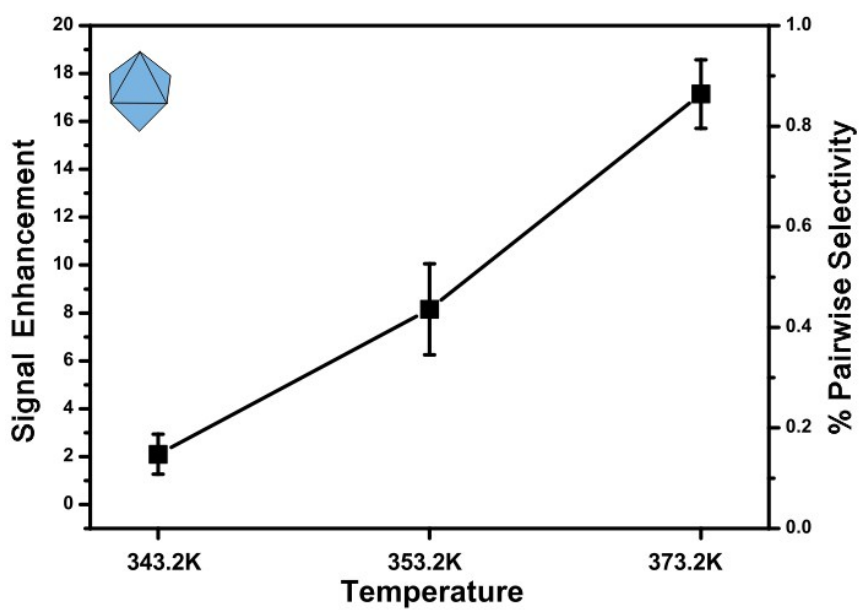


Figure S8. ^1H NMR signal enhancement factor and p- H_2 pairwise selectivity for the hydrogenation of MBY to MBE on Pd OCT-27 catalyst at different reaction temperatures.

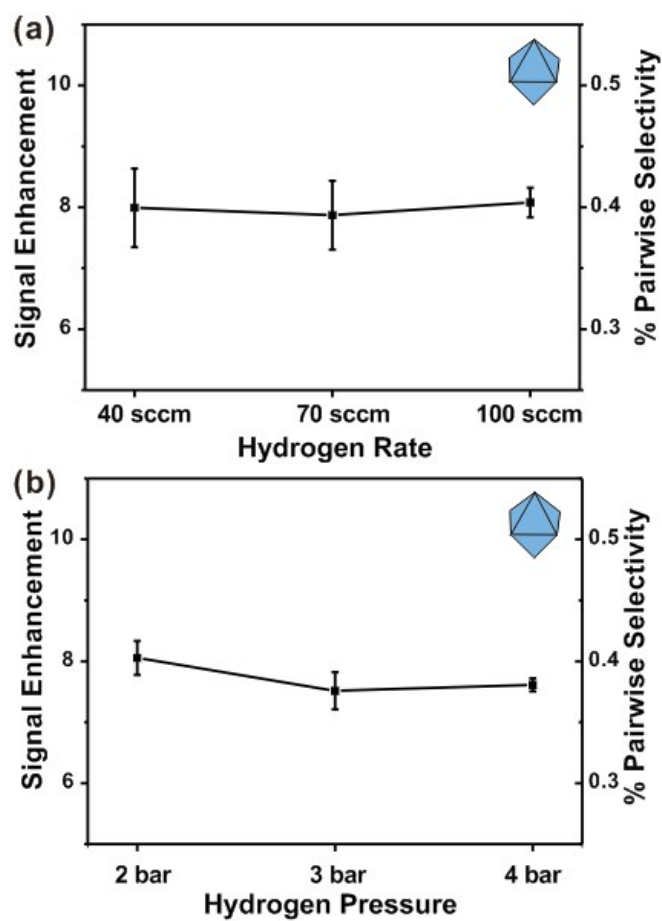


Figure S9. ^1H NMR signal enhancement factor and p- H_2 pairwise selectivity for the hydrogenation of MBY to MBE on Pd OCT-27 catalyst under (a) different p- H_2 flow rate, and (b) different p- H_2 pressure. The reaction temperature is 353 K.

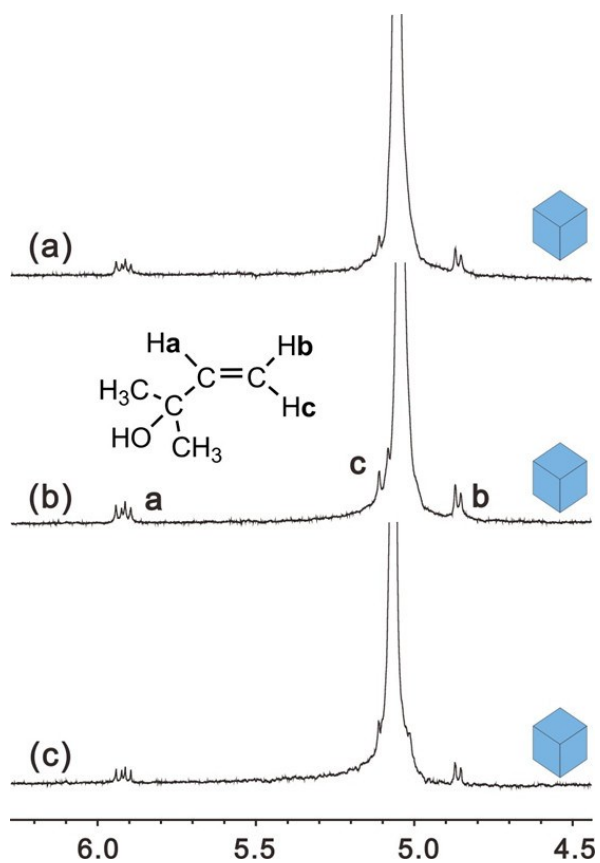


Figure S10. ^1H NMR spectra of products obtained from MBY hydrogenation over cubic Pd nanocrystals with different sizes (a) CUB-8, 8.7 nm, (b) CUB-11, 11.1 nm and (c) CUB-14, 14.4 nm. The spectra is recorded at 353K.

Table S1. Statistics of surface atoms on the Pd nanocrystals.

sample	d_p [nm]	surface statistics			
		D^a [%]	x_{111}^b [%]	x_{100}^b [%]	x_{edge}^b [%]
CUB-8	8.7 nm	12.1	-	80.3	11.4
CUB-11	11.1 nm	9.7	-	84.0	9.3
CUB-14	14.4 nm	7.7	-	87.3	7.5
OCT-17	17.9 nm	8.6	79.2	-	12.4
OCT-27	27.9 nm	5.7	86.1	-	8.3
OCT-34	34.3 nm	4.7	88.5	-	6.8
COT-19	19.4 nm	5.8	67.5	14.6	10.7
TOT-23	23.6 nm	n.d.	n.d.	n.d.	n.d.

^aDispersion (%), defined as the ratio of the number of surface atoms (N_S) to the total number of atoms (N_T). ^bFraction of surface atoms of a given type, $x_i = N_i/N_S$. n.d. indicates the value is not determined. The statistics of surface atoms was based on a nonideal model⁸.

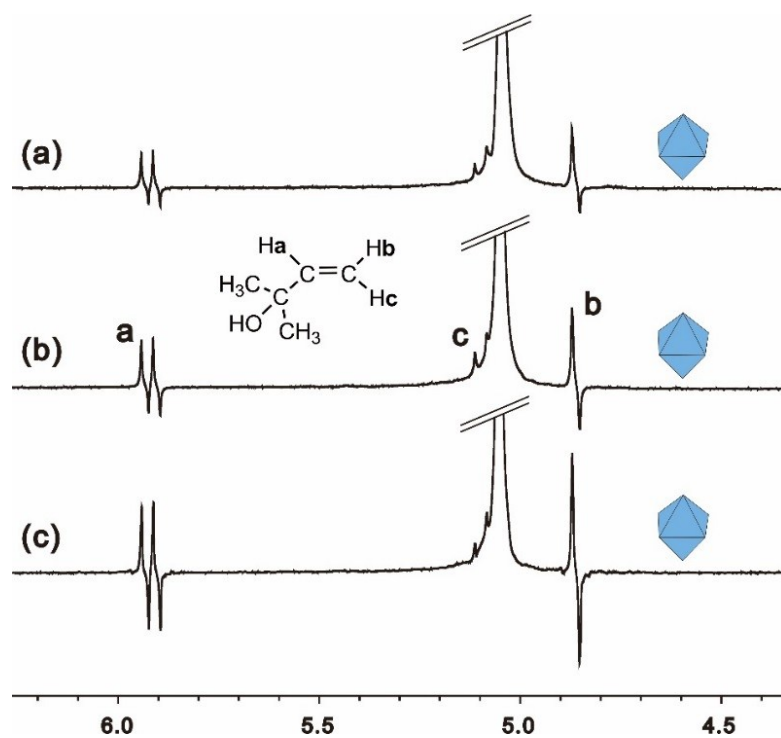


Figure S11. ^1H NMR spectra of products obtained from MBY hydrogenation over Pd octahedrons with different sizes (a) OCT-17, 17.9 nm, (b) OCT-27, 27.9 nm, (c) OCT-34, 34.3 nm. The spectra is recorded at 353K.

References

1. (a)M. S. Jin, H. Zhang, Z. X. Xie and Y. N. Xia, *Energy Environ. Sci.*, 2012, **5**, 6352-6357; (b)M. S. Jin, H. Y. Liu, H. Zhang, Z. X. Xie, J. Y. Liu and Y. N. Xia, *Nano Res.*, 2011, **4**, 83-91.
2. J. Bargon, J. Kandels and K. Woelk, *Z. Phys. Chem.*, 1993, **180**, 65-93.
3. K. V. Kovtunov, V. V. Zhivonitko, I. V. Skovpin, D. A. Barskiy and I. V. Koptug, *Top.Curr. Chem.*, 2013, **338**, 123-180.
4. S. B. Duckett and R. E. Mewis, *Acc. Chem. Res.*, 2012, **45**, 1247-1257.
5. K. V. Kovtunov and I. V. Koptug, in *Magnetic Resonance Microscopy*, Wiley-VCH Verlag GmbH & Co. KGaA, 2009, DOI: 10.1002/9783527626052.ch7, pp. 99-115.
6. D. A. Barskiy, O. G. Salnikov, K. V. Kovtunov and I. V. Koptug, *J. Phys. Chem A*, 2015, **119**, 996-1006.
7. C. R. Bowers, in *eMagRes*, John Wiley & Sons, Ltd, 2007, DOI: 10.1002/9780470034590.emrstm0489.
8. R. Van Hardeveld and F. Hartog, *Surf. Sci.*, 1969, **15**, 189-230.